



HAL
open science

Low torsional barrier challenges in the microwave spectrum of 2,4-dimethylanisole

Lynn Ferres, Wolfgang Stahl, Ha Vinh Lam Nguyen

► **To cite this version:**

Lynn Ferres, Wolfgang Stahl, Ha Vinh Lam Nguyen. Low torsional barrier challenges in the microwave spectrum of 2,4-dimethylanisole. *Journal of Chemical Physics*, 2019, 151 (10), pp.104310. 10.1063/1.5116304 . hal-03183052

HAL Id: hal-03183052

<https://hal.u-pec.fr/hal-03183052>

Submitted on 26 Mar 2021

HAL is a multi-disciplinary open access archive for the deposit and dissemination of scientific research documents, whether they are published or not. The documents may come from teaching and research institutions in France or abroad, or from public or private research centers.

L'archive ouverte pluridisciplinaire **HAL**, est destinée au dépôt et à la diffusion de documents scientifiques de niveau recherche, publiés ou non, émanant des établissements d'enseignement et de recherche français ou étrangers, des laboratoires publics ou privés.

Low torsional barrier challenges in the microwave spectrum of 2,4-dimethylanisole

EP

Cite as: J. Chem. Phys. **151**, 104310 (2019); <https://doi.org/10.1063/1.5116304>

Submitted: 24 June 2019 . Accepted: 08 August 2019 . Published Online: 13 September 2019

Lynn Ferres , Wolfgang Stahl , and Ha Vinh Lam Nguyen 

COLLECTIONS

 This paper was selected as an Editor's Pick



View Online



Export Citation



CrossMark

ARTICLES YOU MAY BE INTERESTED IN

Imaging the nonreactive collisional quenching dynamics of NO ($A^2\Sigma^+$) radicals with O_2 ($X^3\Sigma_g^-$)

The Journal of Chemical Physics **151**, 104304 (2019); <https://doi.org/10.1063/1.5109112>

Direct diabaticization and analytic representation of coupled potential energy surfaces and couplings for the reactive quenching of the excited $2^2\Sigma^+$ state of OH by molecular hydrogen

The Journal of Chemical Physics **151**, 104311 (2019); <https://doi.org/10.1063/1.5111547>

The ground state, quadrupole-bound anion of succinonitrile revisited

The Journal of Chemical Physics **151**, 101101 (2019); <https://doi.org/10.1063/1.5114617>

Lock-in Amplifiers up to 600 MHz

starting at

\$6,210



 Zurich
Instruments

Watch the Video



Low torsional barrier challenges in the microwave spectrum of 2,4-dimethylanisole

Cite as: J. Chem. Phys. 151, 104310 (2019); doi: 10.1063/1.5116304

Submitted: 24 June 2019 • Accepted: 8 August 2019 •

Published Online: 13 September 2019



View Online



Export Citation



CrossMark

Lynn Ferres,¹  Wolfgang Stahl,¹  and Ha Vinh Lam Nguyen^{2,a)} 

AFFILIATIONS

¹Institute of Physical Chemistry, RWTH Aachen University, Landoltweg 2, D-52074 Aachen, Germany

²Laboratoire Interuniversitaire des Systèmes Atmosphériques (LISA), CNRS UMR 7583, Université Paris-Est Créteil, Université de Paris, Institut Pierre Simon Laplace, 61 avenue du Général de Gaulle, F-94010 Créteil, France

^{a)} Author to whom correspondence should be addressed: lam.nguyen@lisa.u-pec.fr

ABSTRACT

Low barriers to internal rotations are especially challenging for both the experimental and theoretical determinations because they result in large tunneling splittings which are hard to assign and in potential functions that can be difficult to model. In the present work, the internal rotations of two methyl groups of 2,4-dimethylanisole were analyzed and modeled using a newly developed computer code, called *ntop*, adapted for fitting the high-resolution torsion-rotation spectra of molecules with two or more methyl rotors. The spectrum was measured using a pulsed molecular jet Fourier transform microwave spectrometer operating in the frequency range of 2.0–26.5 GHz, revealing internal rotation tunneling quintets with splittings of up to several gigahertz. The V_3 potential barriers are 441.139(23) cm^{-1} and 47.649(30) cm^{-1} for the *o*- and *p*-methyl groups, respectively. Quantum chemical calculations predicted only one conformer with the methoxy group in the *anti* position related to the neighboring *o*-methyl group. While the results from geometry optimizations were reliable, *ab initio* calculations at the MP2 level did not reproduce the low torsional barriers, calling for further experiments on related systems and additional theoretical models.

Published under license by AIP Publishing. <https://doi.org/10.1063/1.5116304>

I. INTRODUCTION

Large amplitude motions (LAMs) arising from hindered internal rotations are an important feature in structural chemistry. Among experimental methods, the investigation of the pure rotational spectrum in the microwave region provides the most accurate description of the molecular structure, because the primary spectroscopic data deduced from these spectra, the rotational constants, depend on the mass distribution within the molecules. For terminal methyl groups, the internal rotation effects cause tunneling splittings of the rotational energy levels, from which the potential barriers can be determined precisely. This method has been applied extensively for many molecules with one methyl rotor hindered by a three-fold barrier, which occurs when the methyl top is attached to a molecular frame of C_1 or C_s symmetry.

Some investigations on molecules undergoing internal rotations of two methyl tops were performed. However, such coupled LAMs are much less studied in the literature. The classical examples are acetone,^{1,2} dimethyl ether,^{3,4} and methyl acetate.⁵ Some dimethyl

substituted aromatic systems such as 2,5-dimethylthiophene,⁶ 2,5-dimethylfuran,⁷ and dimethylbenzaldehyde⁸ were also investigated. One of the reasons for this limited number of studies is that the spectra of such molecules are hard to assign and to predict. Furthermore, new theoretical tools involving effective Hamiltonians often have to be developed in order to reproduce the experimental spectra.

We recently started a systematic investigation on dimethyl substituted anisoles^{9,10} and report here the results for the coupled internal rotations determined from the microwave spectrum of 2,4-dimethylanisole (24DMA). While anisole is a rigid backbone molecular system, for which the detection of the rotational spectrum is relatively simple,¹¹ the presence of low barrier(s) to internal rotation by introducing methyl substituent(s) on the phenyl ring produces large splittings in the order of several gigahertz of the rotational levels. This renders the spectral assignment and analysis considerably challenging.

Several computer programs are commonly used for fitting rotational spectra. Currently, the vast majority of rotational spectra

can be analyzed by *SPFIT/SPCAT* included in the program suite *CALPGM* written by Pickett.¹² Further general fitting programs for rotational spectroscopy are available at the “Programs for ROtational SPEctroscopy” (PROSPE)¹³ website. Among them, several programs, e.g., *XIAM* written by Hartwig,¹⁴ can handle the effects of internal rotation up to three internal rotors, which are typically methyl groups. If the barrier to internal rotation is low, higher order perturbation effects often have to be considered, as included in two-top programs written by Ohashi,¹⁵ Kleiner,¹⁶ Groner,¹⁷ and Ilyushin.¹ We wrote a new internal rotation program, called *ntop*, for fitting torsion-rotation spectra of molecules with: (i) n inequivalent or equivalent methyl rotors (the number of rotors n can be adjusted to the value required), (ii) three-fold or six-fold barriers, and (iii) C_{2v} , C_s , or C_1 symmetry at equilibrium. In the present paper, *ntop* is used for fitting the microwave spectrum of 24DMA as a first test of application to a molecule with two inequivalent methyl tops, three-fold barriers, and C_s symmetry at equilibrium.

The methylanisole family with its three isomers *o*-, *m*-, and *p*-methylanisole^{18–20} has already been studied by using microwave spectroscopy. The barrier height of the methyl rotor varies in a wide range, depending on the methyl position. Therefore, it is interesting to compare the barriers of the monomethylanisoles with those of 24DMA to understand the dependence of coupled LAMs in aromatic systems.

II. THEORETICAL SECTION

A. Quantum chemical calculations

If not stated otherwise, all quantum chemical calculations were performed using the *GAUSSIAN* program package (Ref. 21) at the MP2/6-311++G(d,p) level of theory. For a conformational analysis, the dihedral angle $\gamma = \angle(C_2, C_1, O_{14}, C_{15})$ was varied in a grid of 10° , corresponding to a rotation about the C_1 - O_{14} bond, while all other geometry parameters were optimized. The obtained energy points were parameterized by a Fourier expansion with the coefficients given in Table S1 in the [supplementary material](#). The potential energy curve is plotted in Fig. 1. It indicates only one energy minimum at $\gamma = 180^\circ$. The geometry of this minimum was reoptimized under full geometry relaxation, yielding the only stable conformer of 24DMA with all heavy atoms located in plane, as illustrated in Fig. 1. The Cartesian coordinates are available in Table S2 in the [supplementary material](#). Due to steric hindrance, the methoxy group favors an *anti* position relative to the *o*-methyl group. The predicted rotational constants are $A = 2410.28$ MHz, $B = 961.89$ MHz, and $C = 696.54$ MHz. The calculated dipole moment components of $\mu_a = 0.26$ D, $\mu_b = -1.07$ D, and $\mu_c = 0.01$ D imply strong *b*-type, weak *a*-type, and no *c*-type transitions in the microwave spectrum. Frequency calculations indicate one imaginary frequency, which describes the bending motion of the phenyl ring. It is well-known that the MP2/6-311++G(d,p) level of theory often yields an imaginary frequency for stable planar ring systems, which has been reported for benzene and arene.²²

To calculate the barriers to internal rotation of the ring methyl groups at the *para* and *ortho* positions, the dihedral angles $\alpha = \angle(C_5, C_4, C_{19}, H_{22})$ and $\beta = \angle(C_1, C_2, C_{10}, H_{12})$, respectively, were each varied in a grid of 10° , while all other coordinates were optimized at

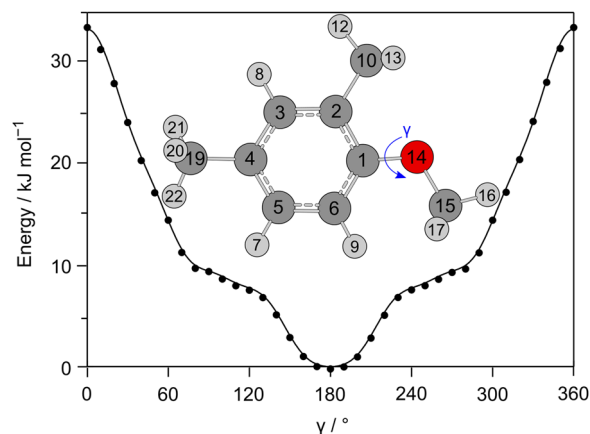


FIG. 1. The potential energy curve of 24DMA obtained by rotating the methoxy group about the C_1 - O_{14} bond by varying the dihedral angle $\gamma = \angle(C_2, C_1, O_{14}, C_{15})$ in a grid of 10° at the MP2/6-311++G(d,p) level of theory. The relative energies are given with respect to the lowest energy conformation with $E = -424.245\,216\,3$ Hartree. Only one minimum exists at $\gamma = 180^\circ$. Inset: The only conformer of 24DMA obtained under full geometry optimizations at the same level of theory.

the MP2/6-311++G(d,p) and B3LYP/6-311++G(d,p) levels of theory. For the *p*- and the *o*-methyl group, threefold torsional potentials were obtained, as illustrated in Figs. 2 and 3, respectively. The Fourier coefficients of these potential energy curves are available in Table S3 in the [supplementary material](#).

For the *p*-methyl group, a discrepancy between the two methods was found. The value of α at the energetic minima optimized with MP2 is $\pm 19.69^\circ$, while it is almost zero in B3LYP calculations (see Fig. 2). Consequently, MP2 states that the equilibrium geometry of 24DMA is C_1 , as can be recognized by the hydrogen positions of

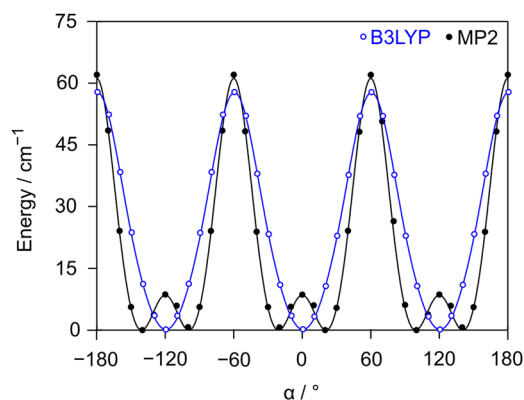


FIG. 2. Threefold torsional potentials obtained by varying the dihedral angle $\alpha = \angle(C_5, C_4, C_{19}, H_{22})$, corresponding to the internal rotation of the *p*-methyl group. Calculations were carried out using the MP2 and B3LYP methods with the 6-311++G(d,p) basis set. Energies relative to the lowest conformations with their absolute energies of $E = -424.245\,216\,3$ Hartree (MP2) and $E = -425.522\,424\,5$ Hartree (B3LYP) are given.

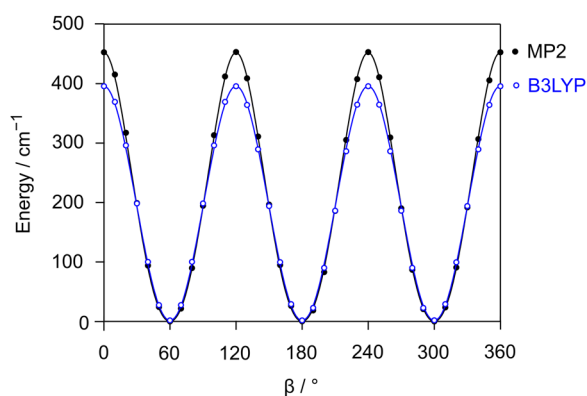


FIG. 3. Threefold torsional potentials obtained by varying the dihedral angle $\beta = \angle(C_1, C_2, C_{10}, H_{12})$, corresponding to the internal rotation of the *o*-methyl group. Calculations were carried out using the MP2 and B3LYP methods with the 6-311++G(d,p) basis set. Energies relative to the lowest conformations with their absolute energies of $E = -424.245\,215\,6$ Hartree (MP2) and $E = -425.522\,424\,3$ Hartree (B3LYP) are given.

the *p*-methyl group in the inset of Fig. 1, whereas B3LYP predicts a C_s structure. The V_6 contribution calculated with the MP2 method is 7.83 cm^{-1} . For this reason, we decide to determine the barrier height by the difference between the optimized minimum and the transition state,²³ which is 61.61 cm^{-1} and 57.68 cm^{-1} for calculations with the MP2 and B3LYP methods, respectively. On the contrary, the two methods are in good agreement in calculations for the *o*-methyl group (Fig. 3). The V_3 potential calculated with the MP2 and the B3LYP method using the transition state is 453.24 cm^{-1} and 393.98 cm^{-1} , respectively.

For the methoxy methyl group of anisole, Reinhold *et al.* reported a barrier to internal rotation of about 1200 cm^{-1} .¹¹ Therefore, a barrier of over 1000 cm^{-1} is also expected for 24DMA. Previous investigations on the three isomers of monomethylanisole^{18–20} as well as on 2,3-⁹ and 3,4-dimethylanisole¹⁰ evidenced that torsional splittings arising from the methoxy methyl group are not resolvable with our experimental resolution and can be neglected.

B. Symmetry considerations

The appropriate molecular symmetry group for a molecule with two inequivalent methyl groups exhibiting internal rotation and C_s point-group symmetry at equilibrium is G_{18} . The assumption of C_s point-group symmetry requires the internal rotation axes of both methyl groups to lie in the plane of symmetry at equilibrium. Recently, we introduced a labeling scheme for 3,4-dimethylanisole, for which G_{18} is written as the semidirect product $(C_3^I \otimes C_3^I) \otimes C_s$.¹⁰ The direct product $C_3^I \otimes C_3^I$ of the two intrinsic (superscript I) C_3 groups of the internal rotors, which is an invariant subgroup of G_{18} , decomposes into five orbits (σ_1, σ_2) under C_s . One representative of each orbit forms the first part of the symmetry label, e.g., (10). The numbers $\sigma = 0, 1$, and 2 represent the three symmetry species A, E_a , and E_b , respectively, of the C_3 group. They correspond to the transformation properties of the C_3 -adapted planar rotor wave functions $e^{i(3k+\sigma)\alpha}$ with $k \in \mathbb{Z}$ and the torsional

angle α . If the quantum numbers K_a and K_c are known, the torsional states can be labeled conveniently by the first part (σ_1, σ_2) of the full symmetry label given in Table 1 of Ref. 10. This abbreviated notation will also be used for 24DMA, which obeys the same nuclear spin statistics and selection rules as those of 3,4-dimethylanisole.¹⁰ For 24DMA, σ_1 and σ_2 represent the *o*- and *p*-methyl groups, respectively.

C. The *ntop* code

The *ntop* code is based on a molecular model consisting of a rigid asymmetric frame and n rigid symmetric tops. Here, we will focus on the $n = 2$ case but in general molecules with more than 2 tops can also be treated with *ntop*. The Hamiltonian, which refers to the principal axis system, will be written as given in Ref. 24

$$H = \frac{1}{2} \mathbf{P}^\dagger \mathbf{I}^{-1} \mathbf{P} + V(\alpha_1, \alpha_2) + H_{ho} \quad (1)$$

with the $n + 3$ dimensional (transposed) angular momentum vector

$$\mathbf{P}^\dagger = (P_a, P_b, P_c, p_1, p_2) \quad (2)$$

and the inertia tensor

$$\mathbf{I} = \begin{pmatrix} I_a & 0 & 0 & \lambda_{i_1 a} I_{\alpha_1} & \lambda_{i_2 a} I_{\alpha_2} \\ 0 & I_b & 0 & \lambda_{i_1 b} I_{\alpha_1} & \lambda_{i_2 b} I_{\alpha_2} \\ 0 & 0 & I_c & \lambda_{i_1 c} I_{\alpha_1} & \lambda_{i_2 c} I_{\alpha_2} \\ \lambda_{i_1 a} I_{\alpha_1} & \lambda_{i_1 b} I_{\alpha_1} & \lambda_{i_1 c} I_{\alpha_1} & I_{\alpha_1} & 0 \\ \lambda_{i_2 a} I_{\alpha_2} & \lambda_{i_2 b} I_{\alpha_2} & \lambda_{i_2 c} I_{\alpha_2} & 0 & I_{\alpha_2} \end{pmatrix}. \quad (3)$$

P_a, P_b, P_c are the components of the overall angular momentum, p_1, p_2 are the angular momenta of the internal rotation of top 1 and 2, respectively, I_a, I_b, I_c are the principal moments of inertia of the entire molecule, $I_{\alpha_1}, I_{\alpha_2}$ are the moments of inertia of top 1 and 2, respectively, $\lambda_{i_1 a}, \lambda_{i_1 b}, \lambda_{i_1 c}$ are the direction cosines between the internal rotor axis i_1 of top 1 and the principal axes a, b , and c , and $\lambda_{i_2 a}, \lambda_{i_2 b}, \lambda_{i_2 c}$ are the direction cosines corresponding to top 2. $V(\alpha_1, \alpha_2)$ is the torsional potential written as a n -dimensional Fourier expansion depending on the torsional angles α_1, α_2 . The Hamiltonian term H_{ho} contains all higher order terms beyond the rigid frame-rigid top model like centrifugal distortion which are added in the usual way and will not be discussed here in detail.

After the inertia tensor is set up, it is inverted numerically. In frequency units, the inverted tensor is given by

$$\frac{1}{2} \mathbf{I}^{-1} = \begin{pmatrix} A' & Z_{ab} & Z_{ac} & Q_{a1} & Q_{a2} \\ Z_{ab} & B' & Z_{bc} & Q_{b1} & Q_{b2} \\ Z_{ac} & Z_{bc} & C' & Q_{c1} & Q_{c2} \\ Q_{a1} & Q_{b1} & Q_{c1} & F_1 & F_{12} \\ Q_{a2} & Q_{b2} & Q_{c2} & F_{12} & F_2 \end{pmatrix}. \quad (4)$$

On the diagonal are the *effective* rotational constants of the entire molecule A', B', C' and of the two internal rotors F_1, F_2 . F_{12} is associated with the kinetic interaction term between top 1 and

top 2. Q_{gi} with $g = a, b, c$ and $i = 1, 2$ are Coriolis-like interaction terms between the overall rotation and the internal rotation, and $Z_{gg'}$ with $g, g' = a, b, c$ arise as a rotation of the coordinate system under the influence of internal rotation.

With Eqs. (1)–(4), the Hamiltonian can be written as

$$\mathbf{H} = \mathbf{H}_r + \mathbf{H}_t + \mathbf{H}_{rt} + \mathbf{H}_{ii} + \mathbf{H}_{ho} \quad (5)$$

with

$$\mathbf{H}_r = A'P_a^2 + B'P_b^2 + C'P_c^2 + \sum_{g \neq g'} Z_{gg'} \{P_g, P_{g'}\}, \quad (6)$$

$$\mathbf{H}_t = \sum_i \left(F_i p_i^2 + \frac{V_{3i}}{2} (1 - \cos 3\alpha_i) + \dots \right), \quad (7)$$

$$\mathbf{H}_{rt} = 2 \sum_{g,i} Q_{gi} P_g p_i, \quad (8)$$

$$\mathbf{H}_{ii} = 2F_{12} p_1 p_2 + V_{12} \cos 3\alpha_1 \cos 3\alpha_2 + V'_{12} \sin 3\alpha_1 \sin 3\alpha_2 + \dots \quad (9)$$

In a first step, the matrix of the pure torsional Hamiltonian \mathbf{H}_t is set up for each top in its respective torsional state σ using the plane wave basis,

$$\psi_i = \sqrt{\frac{1}{2\pi}} e^{i(3k_i + \sigma_i)\alpha_i}.$$

The basis is cut off at a certain $k = k_{max}$, where $k_{max} = 8$ turned out to be sufficient in most cases. After diagonalizing the Hamiltonian matrices, in a second step, the product of the basis functions of the individual tops is used to set up the matrix of $\mathbf{H}_{ii} + \mathbf{H}_t$, where \mathbf{H}_{ii} describes the kinetic top-top interaction as well as the potential coupling terms. Here, the torsional eigenvalues obtained before are simply added on the diagonal. Also, in this step, the basis function v_i is truncated at a certain maximum value v_{max} .

Finally, in a third step, a product basis consisting of the basis functions v_{it} obtained from the previous step up to a maximum value $v_{it,max}$ and the symmetric top functions are used to diagonalize the complete Hamiltonian including the pure rotational part \mathbf{H}_r .

The truncation parameters k_{max} , v_{max} , and $v_{it,max}$ were increased until convergence of the fit was achieved.

III. EXPERIMENTAL SECTION

A. Measurements

The substance with a stated purity of 97% was purchased from Sigma Aldrich, Taufkirchen, Germany, and was used without further purification. A 7 cm piece of the pipe cleaner was soaked with the substance and inserted into a stainless steel tube placed upstream of the nozzle. Helium was used as a carrier gas. The 24DMA-He mixture entered the vacuum chamber under a backing pressure of 200 kPa.

All spectra were recorded using a supersonic jet Fourier transform microwave spectrometer operating in the frequency range from 2 to 26.5 GHz.²⁵ At first, a broadband survey was recorded from 10.0 to 14.0 GHz. The lines observed in the stepped scan were remeasured at a higher resolution, appearing as doublets, due to the Doppler effect. The instrumental linewidth (HWHM)

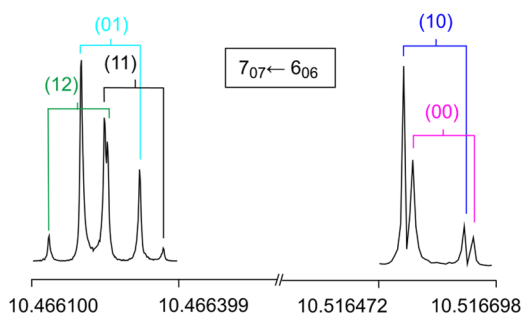


FIG. 4. Two typical spectra of the a -type $7_{07} \leftarrow 6_{06}$ transition of 24DMA which splits into the (00), (10), (01), (11), and (12) torsional species. The frequency is in gigahertz. The Doppler doublets are marked by brackets. For each of these spectra, 400 free induction decays were coadded prior to Fourier transformation. The polarization frequency is 10.46625 GHz for the spectrum at the left hand side and 10.51650 GHz for that at the right hand side.

is 2 kHz.²⁶ The measurement accuracy for 24DMA is about 4 kHz due to line broadening from unresolved splittings arising from the internal rotation of the methoxy methyl group as well as spin-spin and spin-rotation coupling of the hydrogen atoms. Two typical spectra recorded at high resolution and the broadband survey are given in Figs. 4 and 5, respectively.

B. Spectrum assignment and fits

Some rigid rotor b -type transitions from the R -branches $K_a = 1 \leftarrow 0$ and $K_a = 0 \leftarrow 1$ with $J = 6, 7$, and 8 in the broadband survey were first assigned and the three rotational constants could be fitted preliminarily. The (00) and (10) torsional species arising from the internal rotation of the o -methyl group were assigned straightforwardly, because the splittings are very narrow and both components could be captured together in a single high resolution measurement. The number of a - and b -type lines was gradually

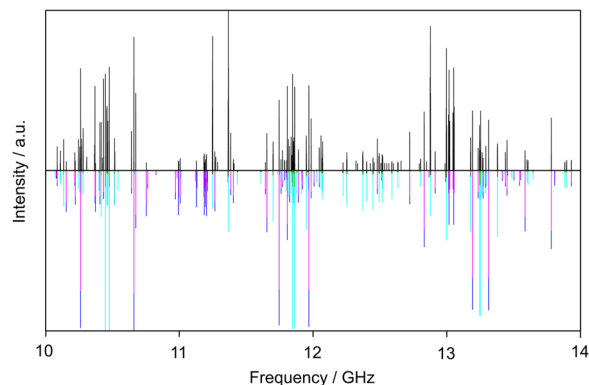


FIG. 5. The broadband survey of 24DMA from 10 to 14 GHz. The experimental spectrum is the upper trace. The lower trace displays the theoretical spectrum (with the color code used in Fig. 4) predicted using the molecular parameters obtained from Fit XIAM given in Table I.

increased until about 50 (00) and 50 (10) transitions were included in a fit with a standard deviation of about 4 kHz for a torsional barrier of about 440 cm^{-1} .

The assignment of the torsional splittings arising from the *p*-methyl group was much more challenging because the barrier to internal rotation is low and starting values predicted by quantum chemical calculations were not sufficiently accurate. Nevertheless, the *a*- and *b*-type transitions could be assigned and finally also some rigid-rotor forbidden but LAM perturbation-allowed *c*-type transitions. In total, 583 torsional species lines were identified and fitted to a standard deviation of 24.1 kHz using the program *XIAM*.¹⁴ The fitted parameters are three rotational constants, five quartic centrifugal constants, and three higher order parameters for the *p*-methyl rotor $D_{pi2J,2}$, $D_{pi2K,2}$, and $D_{pi2-,2}$, which multiply $2(p_2 - \bar{p}^\dagger \bar{P})^2 \bar{P}^2$,

$\{(p_2 - \bar{p}^\dagger \bar{P})^2, P_a^2\}$, and $\{(p_2 - \bar{p}^\dagger \bar{P})^2, (P_b^2 - P_c^2)\}$, respectively. The anti-commutator of two operators is marked by curly brackets. None of the three higher order parameters describing the *o*-methyl rotation could be fitted. The molecular parameters are listed as Fit *XIAM* in Table I. A list of all fitted frequencies along with their deviations is available in Table S4 in the [supplementary material](#).

We then applied the *ntop* code to the same data set. For the low barrier rotor, three additional parameters V_J multiplying $P^2(1 - \cos(3\alpha))$, V_K multiplying $P_a^2(1 - \cos(3\alpha))$, and V_- multiplying $(P_b^2 - P_c^2)(1 - \cos(3\alpha))$ decreased the standard deviation to 4.2 kHz. Fitting the potential coupling term V_{12} multiplying $\cos 3\alpha_1 \cdot \cos 3\alpha_2$ was necessary. The *ntop* fit is summarized as Fit *ntop* in Table I. The deviations are also listed in Table S4 in the [supplementary material](#).

TABLE I. Molecular parameters of 24DMA as obtained with the program *XIAM* and *ntop*.

Par. ^a	Unit	Fit <i>XIAM</i>	Fit <i>ntop</i>	Calc.
<i>A</i>	MHz	2 419.119 8(17)	2 411.905(53)	2 420.0 ^b
<i>B</i>	MHz	963.364 03(57)	973.172(54)	958.3 ^b
<i>C</i>	MHz	698.242 77(38)	687.553(99)	695.4 ^b
<i>D_J</i>	kHz	0.016 1(15)	0.011 00(15)	0.014 96 ^b
<i>D_{JK}</i>	kHz	0.036(12)	0.044 1(11)	0.038 42 ^b
<i>D_K</i>	kHz	0.200(51)	0.294 1(49)	0.270 7 ^b
<i>d₁</i>	kHz	−0.005 09(99)	−0.005 704(87)	−0.004 986 ^b
<i>d₂</i>	kHz	−0.001 27(42)	0.000 732(46)	−0.000 742 1 ^b
<i>V_{3,1}</i> ^c	cm ^{−1}	446.65(16)	441.139(23)	453.24 ^d
<i>V_{3,2}</i> ^c	cm ^{−1}	59.012 0(1)	47.649(30)	61.61 ^d
<i>D_{pi2J,1}</i> ^c	MHz		−0.064 11(95)	
<i>D_{pi2K,1}</i> ^c	MHz		0.037 8(45)	
<i>D_{pi2-,1}</i> ^c	MHz		−0.075 52(89)	
<i>D_{pi2J,2}</i> ^c	MHz	2.882(85)	0.099 4(16)	
<i>D_{pi2K,2}</i> ^c	MHz	84.12(40)	0.526 2(34)	
<i>D_{pi2-,2}</i> ^c	MHz	−2.665(82)	−0.724 8(61)	
<i>V₁₂</i>	GHz		−201.83(52)	
<i>V_{J,2}</i> ^c	MHz		1.930(32)	
<i>V_{K,2}</i> ^c	MHz		10.215(70)	
<i>V_{-,2}</i> ^c	MHz		−14.58(13)	
$\angle(i_1, a)$ ^c	deg	62.974(49)	62.753 4(44)	61.50 ^d
$\angle(i_1, b)$ ^c	deg	27.026(49)	26.973 4(5)	28.50 ^d
$\angle(i_1, c)$ ^c	deg	90.00 ^e	90.00 ^e	90.10 ^d
$\angle(i_2, a)$ ^c	deg	178.067 0(2)	178.088 44(13)	177.97 ^d
$\angle(i_2, b)$ ^c	deg	91.933 0(2)	91.935 1(2)	91.74 ^d
$\angle(i_2, c)$ ^c	deg	90.00 ^e	90.00 ^e	88.97 ^d
<i>N</i> ^f		583	583	
σ ^g	kHz	24.1	4.2	

^aAll parameters refer to the principal axis system. Watson's S reduction and I^r representation were used.

^bGround state constants from anharmonic frequency calculations at the B3LYP/6-311++G(d,p) level of theory.

^cRotors 1 and 2 refer to the *o*- and *p*-methyl groups, respectively.

^dFrom geometry calculations at the MP2/6-311++G(d,p) level of theory.

^eFixed due to symmetry.

^fNumber of lines.

^gStandard deviation of the fit.

IV. DISCUSSION

Using the program *XIAM*, the microwave spectrum of the only conformer of 24DMA including 583 torsional transitions was fitted with a standard deviation of 24.1 kHz, yielding accurately determined molecular parameters. All quantum-chemically predicted rotational constants are in very satisfactory agreement with the experimental values (see Table I), including the centrifugal distortion constants predicted from anharmonic frequency calculations at the B3LYP/6-311++G(d,p) level of theory. The ground state rotational constants obtained from these calculations are $A = 2420.0$, $B = 958.3$, and $C = 695.4$ MHz.

A fit of the same data set with the program *ntop* yields a standard deviation of 4.2 kHz. Being about twice the instrumental accuracy of 2 kHz, this is consistent with the molecular line broadening from the unresolved methoxy methyl internal rotation and hydrogen hyperfine structure. Consistently, if the (00) species lines are fitted separately, which often only require a rigid rotor Hamiltonian corrected by quartic centrifugal distortion terms, a standard deviation of 4.5 kHz is obtained. Some combination difference loops were calculated which also indicated residues of about 4 kHz. Therefore, we conclude that the standard deviation of 4 kHz is not due to the lack of parameters in the Hamiltonian.

Similar to the case of *p*-methyl anisole,²⁰ the six-fold contribution in the potential barrier is neglected, even though the calculations at the MP2/6-311++G(d,p) level of theory have suggested some contribution for the *p*-methyl rotor. The *ntop* fit with pure V_3 terms given in Table I states that the use of V_6 terms is not necessary. If the V_6 parameter is fixed to the predicted value, fits with similar quality are obtained, although the standard deviation is slightly higher than that in the fits where V_6 is fixed to zero, indicating that the V_6 contribution cannot be determined from the present data set.

The calculated torsional barriers of the *o*- and *p*-methyl groups are 453.24 cm^{-1} and 61.61 cm^{-1} , respectively, which are in the same order of magnitude of the experimental values, but higher for both rotors (see Table I for comparison). It is remarkable that the barrier heights are significantly different in Fit *XIAM* and Fit *ntop*. This phenomenon is often observed when effective parameters are floated. Because of the strong correlation with V_3 , F_0 was fixed to 160 GHz in both, Fit *XIAM* and Fit *ntop*, which corresponds to $I_a = 3.159\text{ u}\text{\AA}^2$, a value often found for methyl groups in aromatic molecules.

The barrier heights of the *o*- and *p*-methyl tops obtained with *ntop* are $441.139(23)$ and $47.649(30)\text{ cm}^{-1}$, respectively. The first conclusion that can be drawn is that the torsional barriers of the *o*- and *p*-methyl groups do not change significantly compared to the values of the respective monomethylanisoles. The barrier to internal rotation of the *o*-methyl group in *o*-methylanisole¹⁸ (3) is $444.05(41)\text{ cm}^{-1}$ and the one of the *p*-methyl group in *p*-methylanisole²⁰ (9) is $49.6370(1)\text{ cm}^{-1}$ (see Fig. 6 for a better comparison and molecule numbering). This is probably due to the distance between the two ring methyl groups. However, since the potential coupling term V_{12} in *ntop* is needed, the two LAMs are not independent of each other. The barrier height of the *p*-methyl group deduced with *XIAM* is $59.0120(1)\text{ cm}^{-1}$, surprisingly different from that obtained with *ntop* and that of the *p*-methyl group in *p*-methylanisole. Currently, we have no conclusive statement other than it is conceivable that the values of these barrier absorbed effects are not explicitly treated in

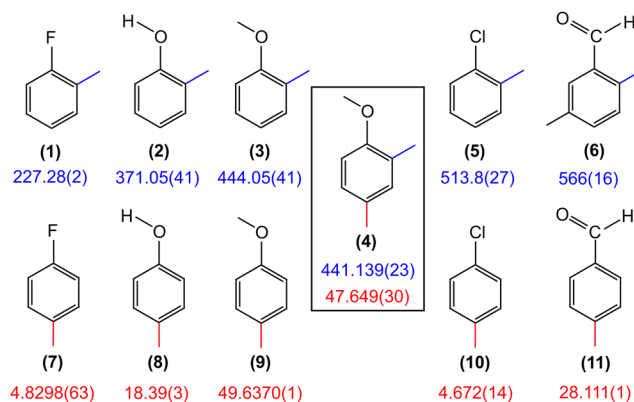


FIG. 6. Torsional barriers in cm^{-1} of the *o*- and *p*-methyl groups in substituted toluene: (1) *o*-Fluorotoluene,²⁷ (2) *anti o*-cresol,²⁸ (3) *o*-methylanisole,¹⁸ (4) 2,4-dimethylanisole (this work), (5) *o*-³⁵Cl-chlorotoluene,²⁹ (6) *syn* 2,5-dimethylbenzaldehyde,⁸ (7) *p*-fluorotoluene,³² (8) *p*-cresol,³⁴ (9) *p*-methylanisole,²⁰ (10) *p*-³⁵Cl-chlorotoluene,³³ and (11) *p*-tolualdehyde.³⁵

XIAM but are accounted for by the additional parameters fitted in *ntop*.

The second conclusion is that the barrier of the *p*-methyl top is by an order of magnitude lower than that of the *o*-methyl top. The latter can be well-explained by steric hindering, because of the bulky methoxy group in the vicinity of the *o*-methyl group. This steric effect is evident in the upper trace of Fig. 6, where the barrier to internal rotation of the *o*-methyl group in *o*-substituted toluene derivatives is compared. The molecules are ordered by increasing hindrance of the *o*-substituent, showing a clearly increasing trend of the potential barrier from (1) to (6).^{18,27–30}

All *p*-substituted toluene derivatives show torsional barriers significantly smaller than the *o*-isomers. As discussed in Ref. 20, there is an intuitive explanation for the low barrier of the ring methyl group in *p*-substituted toluenes. The frame has a perfect C_{2v} symmetry in toluene or in molecules with a symmetric substituent at the *para* position like *p*-fluorotoluene (7) or *p*-chlorotoluene (10). In combination with the local C_{3v} symmetry of the ring methyl group, the V_3 contribution of the potential would be zero and only a small V_6 term exists, which is 4.9 cm^{-1} in the case of toluene,³¹ $4.8298(63)\text{ cm}^{-1}$ for *p*-fluorotoluene (7),³² and $4.872(14)$ for *p*-chlorotoluene (10).³³ If the substituent is slightly asymmetric, such as an alcohol group in *p*-cresol (8),³⁴ a methoxy methyl group in *p*-methylanisole (9)²⁰ and 24DMA (4), or an aldehyde group in *p*-tolualdehyde (11),³⁵ the C_{2v} symmetry of the frame is lowered, causing a V_3 potential term. The smaller the substituent is ($\text{OH} < \text{CHO} < \text{OCH}_3$), the less the C_{2v} symmetry of the frame is broken and consequently the lower the V_3 contribution to the potential becomes [$18.39(3)\text{ cm}^{-1}$ (8)³⁴ $<$ $28.111(1)\text{ cm}^{-1}$ (11)³⁵ $<$ $49.6370(1)\text{ cm}^{-1}$ (9)²⁰ \approx $47.649(30)\text{ cm}^{-1}$ (4), respectively]. In *o*-substituted toluenes, the frame has no longer C_{2v} symmetry. Therefore, the V_3 potential term is dominant and the V_6 potential becomes negligible. We emphasize that all these arguments are intuitive. Searching for the origin of methyl internal barriers remains a challenging task for both experiments and theory for decades, because there are several dependent contributions for

this parameter.³⁶ Systematic quantum chemical calculations including natural bonding orbitals method might help to give evidence for the arguments above.

SUPPLEMENTARY MATERIAL

See [supplementary material](#) for Fourier coefficients, Cartesian coordinates, and frequency lists.

ACKNOWLEDGMENTS

We thank the Land Nordrhein-Westfalen for funds. Simulations were performed with computing resources granted by RWTH Aachen University under project <thes0248>. This work was supported by the Agence Nationale de la Recherche ANR (Project No. ANR-18-CE29-0011).

REFERENCES

- ¹V. V. Ilyushin and J. T. Hougen, *J. Mol. Spectrosc.* **289**, 41 (2013).
- ²P. Groner, S. Albert, E. Herbst, F. C. D. Lucia, F. J. Lovas, B. J. Drouin, and J. C. Pearson, *Astrophys. J., Suppl. Ser.* **142**, 145 (2002).
- ³J. R. Durig, Y. S. Li, and P. Groner, *J. Mol. Spectrosc.* **62**, 159 (1976).
- ⁴H. Lutz and H. Dreizler, *Z. Naturforsch., A* **30**, 1782 (1975).
- ⁵H. V. L. Nguyen, I. Kleiner, S. T. Shipman, Y. Mae, K. Hirose, S. Hatanaka, and K. Kobayashi, *J. Mol. Spectrosc.* **299**, 17 (2014).
- ⁶V. Van, W. Stahl, and H. V. L. Nguyen, *Phys. Chem. Chem. Phys.* **17**, 32111 (2015).
- ⁷V. Van, J. Bruckhuisen, W. Stahl, V. Ilyushin, and H. V. L. Nguyen, *J. Mol. Spectrosc.* **343**, 121 (2018).
- ⁸M. Tudorie, I. Kleiner, M. Jahn, J.-U. Grabow, M. Goubet, and O. Pirali, *J. Phys. Chem. A* **117**, 13636 (2013).
- ⁹L. Ferres, K.-N. Truong, W. Stahl, and H. V. L. Nguyen, *Chem. Phys. Chem.* **19**, 1781 (2018).
- ¹⁰L. Ferres, J. Cheung, W. Stahl, and H. V. L. Nguyen, *J. Phys. Chem. A* **123**, 3497 (2019).
- ¹¹B. Reinhold, I. A. Finneran, and S. T. Shipman, *J. Mol. Spectrosc.* **270**, 89 (2011).
- ¹²H. M. Pickett, *J. Mol. Spectrosc.* **148**, 371 (1991).
- ¹³See <http://info.ifpan.edu.pl/~kisiel/prospe.htm> for fitting programs for rotational spectroscopy.
- ¹⁴H. Hartwig and H. Dreizler, *Z. Naturforsch., A* **51**, 923 (1996).
- ¹⁵N. Ohashi and J. T. Hougen, *J. Mol. Spectrosc.* **203**, 170 (2000).
- ¹⁶M. Tudorie, I. Kleiner, J. T. Hougen, S. Melandri, L. W. Sutikdja, and W. Stahl, *J. Mol. Spectrosc.* **269**, 211 (2011).
- ¹⁷P. Groner, *J. Chem. Phys.* **107**, 4483 (1997).
- ¹⁸L. Ferres, H. Mouhib, W. Stahl, and H. V. L. Nguyen, *ChemPhysChem* **18**, 1855 (2017).
- ¹⁹L. Ferres, W. Stahl, and H. V. L. Nguyen, *J. Chem. Phys.* **148**, 124304 (2018).
- ²⁰L. Ferres, W. Stahl, I. Kleiner, and H. V. L. Nguyen, *J. Mol. Spectrosc.* **343**, 44 (2018).
- ²¹M. J. Frisch, G. W. Trucks, H. B. Schlegel, G. E. Scuseria, M. A. Robb, J. R. Cheeseman, G. Scalmani, V. Barone, B. Mennucci, G. A. Petersson, H. Nakatsuji, M. Caricato, X. Li, H. P. Hratchian, A. F. Izmaylov, J. Bloino, G. Zheng, J. L. Sonnenberg, M. Hada, M. Ehara, K. Toyota, R. Fukuda, J. Hasegawa, M. Ishida, T. Nakajima, Y. Honda, O. Kitao, H. Nakai, T. Vreven, J. A. Montgomery, Jr., J. E. Peralta, F. Ogliaro, M. Bearpark, J. J. Heyd, E. Brothers, K. N. Kudin, V. N. Staroverov, R. Kobayashi, J. Normand, K. Raghavachari, A. Rendell, J. C. Burant, S. S. Iyengar, J. Tomasi, M. Cossi, N. Rega, J. M. Millam, M. Klene, J. E. Knox, J. B. Cross, V. Bakken, C. Adamo, J. Jaramillo, R. Gomperts, R. E. Stratmann, O. Yazyev, A. J. Austin, R. Cammi, C. Pomelli, J. W. Ochterski, R. L. Martin, K. Morokuma, V. G. Zakrzewski, G. A. Voth, P. Salvador, J. J. Dannenberg, S. Dapprich, A. D. Daniels, O. Farkas, J. B. Foresman, J. V. Ortiz, J. Cioslowski, and D. J. Fox, *GAUSSIAN 09*, Revision A.02, Gaussian, Inc., Wallingford, CT, 2009.
- ²²D. Moran, A. C. Simmonett, F. E. Leach, W. D. Allen, P. v. R. Schleyer, and H. F. Schaefer, *J. Am. Chem. Soc.* **128**, 9342 (2006).
- ²³H. B. Schlegel, *J. Comput. Chem.* **3**, 214 (1982).
- ²⁴H. Dreizler, "Mikrowellenspektroskopische Bestimmung von Rotationsbarrieren freier Moleküle," in *Spektren und Molekülbau*, Fortschritte der Chemischen Forschung Vol. 10/1 (Springer, Berlin, Heidelberg, 1968).
- ²⁵J.-U. Grabow, W. Stahl, and H. Dreizler, *Rev. Sci. Instrum.* **67**, 4072 (1996).
- ²⁶J.-U. Grabow and W. Stahl, *Z. Naturforsch., A* **45**, 1043 (1990).
- ²⁷S. Jacobsen, U. Andresen, and H. Mäder, *Struct. Chem.* **14**, 217 (2003).
- ²⁸A. Welzel, A. Hellweg, I. Merke, and W. Stahl, *J. Mol. Spectrosc.* **215**, 58 (2002).
- ²⁹K. P. R. Nair, J. Demaison, G. Wlodarczak, and I. Merke, *J. Mol. Spectrosc.* **237**, 137 (2006).
- ³⁰H. D. Rudolph, K. Walzer, and I. Krutzik, *J. Mol. Spectrosc.* **47**, 314 (1973).
- ³¹H. D. Rudolph, H. Dreizler, A. Saeschke, and P. Z. Wendling, *Z. Naturforsch., A* **22**, 940 (1967).
- ³²J. Rottstegge, H. Hartwig, and H. Dreizler, *J. Mol. Struct.* **478**, 37 (1999).
- ³³G. Herberich, *Z. Naturforsch., A* **22**, 761 (1967).
- ³⁴A. Hellweg and C. Hättig, *J. Chem. Phys.* **127**, 024307 (2007).
- ³⁵H. Saal, J.-U. Grabow, A. R. Hight Walker, J. T. Hougen, I. Kleiner, and W. Caminati, *J. Mol. Spectrosc.* **351**, 55 (2018).
- ³⁶L. Goodman, V. Pophristic, and F. Weinhold, *Acc. Chem. Res.* **32**, 983 (1999).